Further analysis shows that in the case of axisymmetric flow, the scalar momentum equations (obtained from Eq. (19) with the corresponding expression of σ^{ij} substituted therein) cannot be stated in the strong conservation-law forms. In this form some undifferentiated terms appear which act as "sources" of momentum. Vinokur[8] has shown that the same terms appear when the conservation law [Eq. (3)] is applied to a finite-volume element for axisymmetric flow.

Acknowledgment

This research has been supported in part by NASA Marshall Space Flight Center, Contract NAS8-32912.

References

[1]Thompson, J. F., Thames, F. C., and Mastin, C. W., "Automatic Numerical Generation of Body-Fitted Curvilinear Coordinate System for Fields Containing any Number of Arbitrary Two-Dimensional Bodies," *Journal of Computational Physics*, Vol. 15, 1974, pp. 299-319.

[2]Warsi, Z.U.A. and Thompson, J. F., "Machine Solutions of Partial Differential Equations in the Numerically Generated Coordinate Systems," Engineering and Industrial Research Station, Mississippi State University, Rept. MSSU-EIRS-77-1, Aug. 1976.

[3]Eiseman, P. R., "A Coordinate System for a Viscous Transonic Cascade Analysis," *Journal of Computational Physics*, Vol. 26, 1978, pp. 307-338.

[4]Warsi, Z.U.A., Devarayalu, K., and Thompson, J. F., "Numerical Solution of the Navier-Stokes Equations for Arbitrary Blunt Bodies in Supersonic Flows," *Numerical Heat Transfer*, Vol. 1, 1978, pp. 499-516.

[5]Kutler, P., Reinhardt, W. A., and Warming, R. F., "Numerical Computation of Multishocked, Three-Dimensional Supersonic Flow Fields with Real Gas Effects," AIAA Paper 72-702, June 1972.

[6]McVittie, G. C., "A Systematic Treatment of Moving Axes in Hydrodynamics," *Proceedings of Royal Society*, Series A, Vol. 196, 1949, pp. 285-300.

[7]Viviand, H., "Formes Conservatives des Equations de la Dynamique des Gas," *La Recherche Aerospatiale*, No. 1974-1, 1974, pp. 65-66.

[8]Vinokur, M., "Conservation Equations of Gas Dynamics in Curvilinear Coordinate Systems," *Journal of Computational Physics*, Vol. 14, 1974, pp. 105-125.

[9]Truesdell, C. and Toupin, R. A., "The Classical Field Theories," *Handbuch der Physik*, Vol. VIII/I, Springer-Verlag, Berlin, 1960.

[10]Germain, P., "Shock Waves, Jump Relations, and Structure," *Advances in Applied Mechanics*, Vol. 12, 1972, p. 132.

[11]Borisenko, A. I. and Tarapov, I. E., "Vector and Tensor Analysis with Applications," translated by R. A. Silverman, Prentice-Hall, Inc., Englewood Cliffs, N.J., 1968.

[12]Thomas, P. D. and Lombard, C. K., "The Geometric Conservation Law-A Link Between Finite-Difference and Finite Volume Methods of Flow Computation on Moving Grids," AIAA Paper 78-1208, 1978.

AIAA 80-0028R

Supersonic Flow Past Conical Bodies with Nearly Circular Cross Sections

Martin C. Jischke*
University of Oklahoma, Norman, Okla.

Introduction

DOTY and Rasmussen,[1] using a constant-density approximation, have presented accurate, analytical results for hypersonic flow past an inclined cone. Lee and Rasmussen,[2] employing similar approximations that linearize the governing equations, have analyzed hypersonic flow past elliptical cones. It is the purpose of this paper to extend this approach to supersonic flow past cones of more arbitrary cross section.

The analysis uses a straightforward perturbation of supersonic flow past an unyawed cone. As first noted by Ferri,[3] such a procedure fails for cones at yaw or with noncircular cross sections in a thin layer of intense vorticity near the cone called the vortical layer. The solutions obtained herein must, thus, be viewed as the first-order outer expansion in a matched asymptotic expansion scheme and must, in principle, be asymptotically matched to solutions valid in the vortical layer. Investigations by Munson[4] and others, however, have shown that the results obtained for the circumferential velocity and pressure by means of a regular perturbation scheme are uniformly valid throughout the shock layer, a conclusion that extends the use of the present paper.

Analysis

We employ a spherical polar coordinate system (r,θ,ϕ) with origin at the vertex of the cone which is assumed to be embedded in uniform supersonic stream along the cone axis. The cone is assumed to be sufficiently slender that the shock is attached to its pointed nose. The cone cross section is described by means of a Fourier series for the polar angle of the body,

$$\theta_c = \delta + \sum_{n=1} \epsilon_n \cos[n(\phi - \phi_n)]$$

Here δ is the half-angle of the basic circular cone and the ϵ_n parameters that describe the deviation of the cross section from a circle. For example, ϵ_2 measures elliptical eccentricity. The ϕ_n determine the relative phase of the various Fourier components. Our perturbation scheme assumes the ϵ_n are small compared to δ. This representation of the body shape suggests the following form for the shock angle θ_s, the radial velocity u, and the azimuthal velocity w,

$$\theta_s = \beta + \alpha g_0 \cos(\phi - \phi_0) + \sum_{n=1}^{\infty} \epsilon_n g_n \cos[n(\phi - \phi_n)] \quad (1)$$

$$u = u_0(\theta) + \alpha U_0(\theta)\cos(\phi - \phi_0) + \sum_{n=1}^{\infty} \epsilon_n U_n(\theta)\cos[n(\phi - \phi_n)] \quad (2)$$

$$w = \alpha W_0(\theta)\sin(\phi - \phi_0) + \sum_{n=1}^{\infty} \epsilon_n W_n(\theta) n \sin[n(\phi - \phi_n)] \quad (3)$$

The expansions for the polar velocity v, entropy s, sound speed a, and pressure p are identical in form to that for the radial velocity. Lower case quantities refer to the unyawed circular cone flow, a result that is presumed to be known. The angle of attack α is also assumed to be small compared to δ.

Substituting these expansions into the inviscid, adiabatic, compressible flow equations as well as the shock jump relations and tangency condition at the body and then equating powers of α and the ϵ_n to zero gives a hierarchy of problems, the first being that past an unyawed circular cone. The next problem corresponds to the linear effects of angle of attack α and noncircular cross sections ϵ_n and can, after some manipulation, be reduced to the following second-order ordinary differential equation for the radial velocity perturbation $U_n(\theta)$,

$$U_n'' + \cot\theta U_n' + (2 - n^2\csc^2\theta) U_n = n^2 \csc^2\theta F_n(\theta) + G_n \quad (4)$$

Presented as Paper 80-0028 at the AIAA 18th Aerospace Sciences Meeting, Pasadena, Calif., Jan. 14-16, 1980; submitted Feb. 8, 1980; revision received July 28, 1980.

*Professor and Director, School of Aerospace, Mechanical, and Nuclear Engineering. Associate Fellow AIAA.

where

$$F_n(\theta) = \frac{S_n}{\gamma(\gamma-1)} (-v_0\sin\theta)^{1/2} a_0^{1/(\gamma-1)} \times \int_\beta^\theta \frac{a_0^{(2\gamma-3)/(\gamma-1)}}{v_0(-v_0\sin\theta)^{1/2}} d\theta \tag{5}$$

$$G_n = \frac{2u_0v_0}{a_0^2} U_n' + \left(\frac{v_0}{a_0}\right)^2 \left[U_n + U_n'' + (\gamma-1)(u_0+v_0') \times \left(\frac{u_0U_n}{a_0^2} + \frac{v_0U_n'}{a_0^2}\right) + \frac{2v_0U_n'}{a_0^2}\right] \tag{6}$$

with boundary conditions that derive from the shock jump relations,

$$\theta=\beta: \quad U_n = -g_n(u_0' + \sin\theta) \tag{7}$$

$$U_n' = -g_n\left[v_0' + v_0\cot\theta\frac{2-(\gamma-1)K_\theta^2}{2+(\gamma-1)K_\theta^2}\right] \tag{8}$$

and the tangency condition at the body,

$$\theta=\delta: \quad U_n' = 2u_0 \tag{9}$$

Here γ is the constant ratio of specific heats and $K_\theta = M_1\theta$. Analysis shows that the entropy perturbation function S_n is constant. As the results for the case $n=0$ can be obtained directly from those for the case $n=1$, we shall not write the special form of Eqs. (4-9) for $n=0$.

Equation (4) is a linear equation for U_n that we propose to solve approximately by ignoring G_n. Specifically, G_n is proportional to v_0/a_0 and thus vanishes at the cone surface. In addition, when K_δ is large, $(v_0/a_0)^2$ is small at the shock. Thus, for large K_δ, G_n is small everywhere and is negligible. Furthermore, the contribution of G_n to the solution for U_n vanishes identically at the shock because U_n is made to satisfy exactly the boundary conditions there. Consequently, even for K_δ that are not large, the solution obtained by neglecting G_n is a rather accurate one. Of course, a correction to this first approximation can be obtained by evaluating G_n with the first approximation. Calculations by Lee and Rasmussen[2] for the particular case $n=2$ showed that the resulting correction was very small for almost all K_δ.

If we ignore G_n, Eq. (4) becomes the associated Legendre equation and, using the method of variation of parameters, the solution can be written as a quadrature involving the associated Legendre function of the second kind of order one and degree n, $Q_1^n(\theta)$. However, the resulting quadrature cannot be carried out in closed form in terms of known functions. This difficulty is overcome if we restrict attention to slender bodies ($\delta\to 0$) at high Mach numbers ($M_1\to\infty$) such that the hypersonic similarity variable K_δ remains finite. In the hypersonic small disturbance approximation, we have, to a high degree of accuracy,

$$u_0 = 1 - \frac{\delta^2}{2}\left[\frac{K_\theta^2}{K_\delta^2} + 2\ln\frac{K_\beta}{K_\delta}\right] \tag{10}$$

$$v_0 = -\theta[1 - K_\delta^2/K_\theta^2] \tag{11}$$

and F_n can be evaluated explicitly (see Ref. 9 for the result). Equation (4) can then be integrated for the U_n explicitly in closed form in terms of known functions. From these results one can then determine the g_n, V_n, W_n, etc. Reference 9 contains the explicit results for $n=0$, 1, 2, 3, 4. Space limitations prevent displaying the explicit formulas here. There are no essential difficulties to extending the available results to larger n.

Of particular interest is the surface pressure coefficient C_p, which we write in the hypersonic small disturbance theory similarity form,

$$\frac{C_p}{\delta^2} = \frac{c_{p_0}}{\delta^2} + \frac{\alpha}{\delta}\frac{C_{p_0}}{\delta}\cos(\phi-\phi_0) + \sum_n \frac{\epsilon_n}{\delta}\frac{C_{p_n}}{\delta}\cos[n(\phi-\phi_n)] \tag{12}$$

where

$$\frac{c_{p_0}}{\delta^2} = 1 + \frac{(\gamma+1)K_\delta^2+2}{(\gamma-1)K_\delta^2+2}\ln\left(\frac{\gamma+1}{2} + \frac{1}{K_\delta^2}\right) \tag{13}$$

$$\frac{C_{p_n}}{\delta} = -\gamma\left(\frac{c_{p_0}}{\delta^2} + \frac{2}{\gamma K_\delta^2}\right) g_n \times \left\{\frac{4(K_\beta^2-1)^2\delta}{(2\gamma K_\beta^2-\gamma+1)[(\gamma-1)K_\beta^2+2]\beta} + \frac{U_n(\delta)}{\delta g_n}\frac{K_\delta^2}{1+\tfrac{1}{2}(\gamma-1)K_\delta^2[1+2\ln(K_\beta/K_\delta)]}\right\} \tag{14}$$

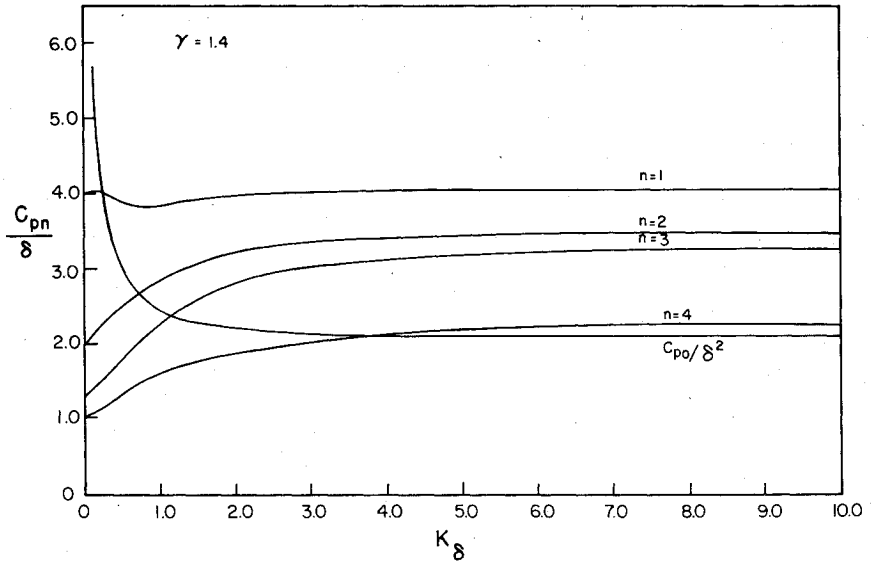

Fig. 1 Surface pressure coefficient, $K_\delta = M_1\delta$.

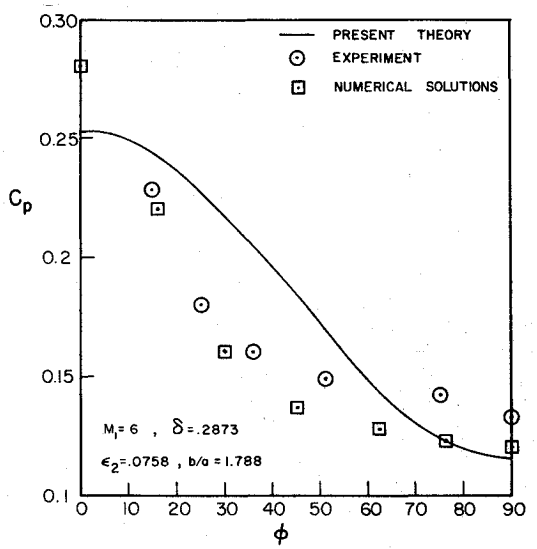

Fig. 2 Elliptical cone: comparison of theory and experiment.

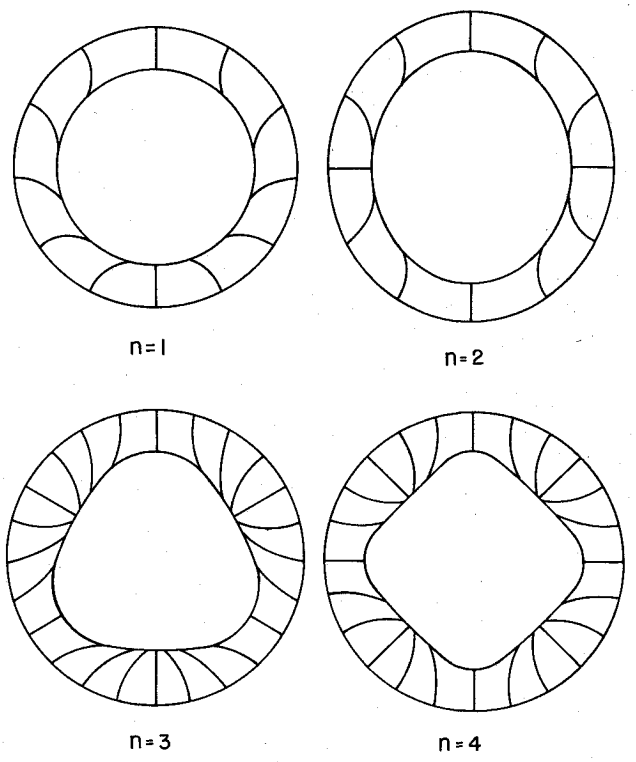

Fig. 3 Cross flow streamlines, $K_\delta = 1$, $\epsilon_n = 0.1$, $\gamma = 1.4$.

Figure 1 shows typical results for c_{p0}/δ^2 and C_{pn}/δ for $\gamma = 1.4$. These results achieve a hypersonic limiting value as $K_\delta \to \infty$, which agrees well with other known solutions. For example, our result for C_{pl}/δ takes the limiting value 4.046, which is to be compared with 4.088 obtained by Cheng[5] in a separate analysis. The linear theory limit, $K_\delta \to 0$, of Eq. (14) yields $C_{pn}/\delta \sim 4/n$, which agrees exactly with the linearized theory result of Mascitti.[6]

Figure 2 shows a typical comparison of the results of the present theory for a slightly elliptical cone ($n=2$) with experimental data of Visich and Zakkay[7] and with a purely numerical calculation due to Jones.[8] As these results show, the present approximate theory faithfully reproduces the azimuthal trends observed experimentally. Other comparisons with less eccentric elliptical cones show an even closer agreement.[9] Comparison of the present theory with experimental results for a circular cone at angle of attack give excellent agreement if α/δ is sufficiently small (e.g., $\alpha/\delta \lesssim 0.4$).[9]

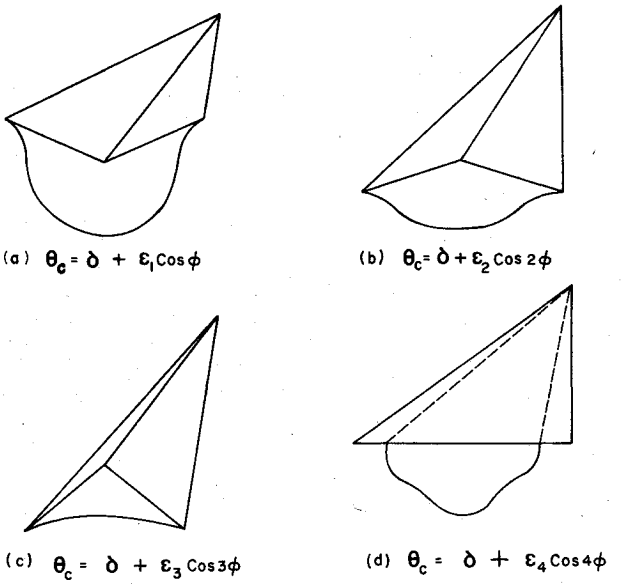

Fig. 4 Waverider geometries.

Streamsurfaces and Waverider Geometries

These analytical results for the velocity field allow us to explicitly determine the streamsurfaces of the flow, e.g., surfaces composed of streamlines. The streamlines follow from solutions of $dr \times V = 0$ where r denotes position along the streamline. Substituting the expansions for u, v, and w into the streamline equation gives two independent scalar equations. One of these equations can be integrated immediately, to lowest order, to give

$$\frac{r}{r_i} = \exp\left(\int_{\theta_i}^{\theta} \frac{u_0}{v_0}\, d\theta\right) \tag{15}$$

Here r_i and θ_i are constants of integration that describe the streamline passing through the point (r_i, θ_i, ϕ_i). Similarly, the second equation becomes

$$\frac{d\theta}{v_0 \sin\theta} = \frac{d\phi}{\alpha W_0(\theta)\sin(\phi - \phi_0) + \sum_{n=1}^{\infty} \epsilon_n W_n(\theta)\, n \sin[n(\phi - \phi_n)]} \tag{16}$$

which cannot be integrated analytically, in general. However, for cones represented by a single Fourier component, a simple result is obtained,

$$\tan\left(\frac{n\phi}{2}\right) = \tan\left(\frac{n\phi_i}{2}\right) \exp\left\{n^2 \epsilon_n \int_{\theta_i}^{\theta} \frac{W_n}{v_0 \sin\theta}\, d\theta\right\} \tag{17}$$

Using Eqs. (10) and (11), we can evaluate the integrals in Eqs. (15) and (17) to obtain, approximately,

$$\frac{r}{r_i} = \left(\frac{\theta_i - \delta^2}{\theta^2 - \delta^2}\right)^{1/2} \tag{18}$$

$$\tan\left(\frac{n\phi}{2}\right) = \tan\left(\frac{n\phi_i}{2}\right) \left(\frac{\theta^2 - \delta^2}{\theta_i^2 - \delta^2} \frac{\theta_i^2}{\theta^2}\right)^{[n^2 \epsilon_n (F_n U_n)_\delta]/2\delta^2} \tag{19}$$

Typical results from Eq. (19) are shown in Fig. 3 for $n = 1$-4. These cross flow streamlines give the projection of streamlines on the unit sphere.

Any streamsurface of an inviscid flow can be taken to be a solid boundary. Consequently, the streamlines shown in Fig. 3 can be used to generate new lifting body shapes. These shapes are called waveriders as they develop lift because of the shock wave they "ride" upon. By choosing streamlines such as shown in Fig. 3, bodies can be developed which have winglike surfaces that fair smoothly into the rest of the body. Closed aerodynamic shapes can be achieved in a variety of ways. Figure 4 shows sketches of possible shapes that derive from the streamlines in Fig. 3 and planes parallel to the freestream velocity. These waveriders efficiently integrate volumetric, propulsive, and aerodynamic requirements and could be the basis for a new generation of maneuverable supersonic/hypersonic vehicles. The analytical solutions developed herein are particularly attractive in that they allow the effects of Mach number, angle of attack, and cross-sectional shapes to be evaluated in closed form.

Acknowledgments

This work was sponsored by the Air Force Office of Scientific Research under AFOSR Grant 77-3468 and by the Air Force Armament Laboratory under Contract F0 8635-79-C-0017. The author has profited from discussions of this work with D. Daniel and M. Rasmussen.

References

[1] Doty, R. T. and Rasmussen, M. L., "Approximation for Hypersonic Flow Past an Inclined Cone," *AIAA Journal*, Vol. 11, Sept. 1973, pp. 1310-1315.

[2] Lee, H. M. and Rasmussen, M. L., "Hypersonic Flow Past an Elliptic Cone," AIAA Paper 79-0364, Jan. 1979.

[3] Ferri, A., "Supersonic Flow Around Circular Cones at Angle of Attack," NACA TN 2236, 1950.

[4] Munson, A. G., "The Vortical Layer on an Inclined Cone," *Journal of Fluid Mechanics*, Vol. 20, 1964, pp. 625-643.

[5] Cheng, H. K., "Hypersonic Flows Past a Yawed Circular Cone and Other Pointed Bodies," *Journal of Fluid Mechanics*, Vol. 12, 1962, pp. 169-191.

[6] Mascitti, V. R., "Calculation of Linearized Supersonic Flow Over Slender Cones of Arbitrary Cross Section," NASA TN D-6818, July 1972.

[7] Zakkay, V. and Visich, M., Jr., "Experimental Pressure Distribution on Conical Elliptic Bodies at $M=3.09$ and 6.0," Polytechnic Institute of Brooklyn, PIBAL Rept. 467, March 1959.

[8] Jones, D. J., "Numerical Solutions of the Flow Field for Conical Bodies in a Supersonic Stream," National Research Council of Canada Aero Rept. LR-507, July 1968.

[9] Jischke, M. C., Rasmussen, M. L., Lee, H. M., Kim, B. S., and Kan, H. W., "Supersonic Lifting Body Aerodynamics," University of Oklahoma AMNE Research Rept. 80-19, Oct. 1980.

AIAA 81-4038

Technique for the Evaluation of Wall Interference at Transonic Speeds

Allan B. Bailey* and Donald G. Miller†
Lawrence Livermore National Laboratory, University of California, Livermore, Calif.

In recent years, there has been an increased emphasis upon the development of more efficient transport configurations with cruise speeds in the transonic speed regime. This has resulted in a requirement for high quality aerodynamic data on increasingly complex configurations in this speed regime. This requirement for high quality data has revealed some of the shortcomings of existing transonic test facilities.

A limitation of existing transonic wind tunnels is their inability to provide an adequate simulation of full-scale free-flight Reynolds number. It has been proposed[1] that this present inadequacy can be overcome by operating transonic wind tunnels at low total temperatures, i.e., on the order of 80 K. In such test facilities, the maximum values of Reynolds number are obtained at the lowest values of total temperature. Under these conditions, the possibility exists that condensation in the tunnel flow can occur with its attendant effects on the aerodynamic measurements.

A second concern in wind tunnel measurements, cryogenic or not, is the manner in which these measurements are affected by the tunnel boundary. Although significant improvements have been made in the theoretical methods that have been developed to correct for these boundary effects, these methods are not yet in a sufficiently developed state where they can be used to correct the aerodynamic measurements for wall interference effects.

From the foregoing, it clearly is necessary to distinguish between wall interference and condensation effects in the operation of cryogenic transonic wind tunnels. It is the purpose of this Note to suggest that some aspects of these problems can be evaluated using existing free-flight sphere drag data, although additional measurements at lower Mach numbers and high Reynolds numbers would be highly desirable.

To properly calibrate a wind tunnel in the transonic region, a known configuration with sufficient real free-flight data is required. The obvious shape is the sphere, since projectile or other shapes require duplicating in the tunnel the complicated yaw, spin, and orientation dependence on M_∞ of free-flight conditions.

In our context, three types of sphere drag data need to be considered. These are 1) actual free-flight data (ff) from firings in aerodynamic ranges; 2) force balance measurements in a wind tunnel (t) using stings; and 3) free-flight firings through a wind tunnel (tff). An equivalent to 3 is the sting-free magnetic suspension technique (tsf) in a wind tunnel. As will be seen, these data do not appear to yield the same results. Consequently data of type 1 can be used both to calibrate tunnel effects on type 3 data and sting effects on type 2 data.

Jaffe[2] has measured the drag of a sphere in a transonic wind tunnel both with a force balance (t) and also with a free-flight technique (tff). As a result of these measurements (Fig. 1), Jaffe[2] observes that sphere drag measurements are not affected significantly by reasonably sized stings. However, it should be noted that the experimental free-flight drag value at $M_\infty \approx 0.95$ is approximately 10% greater than the corresponding force balance value. To determine whether this difference is a result of sting interference effects at this Mach number would require a further experimental investigation. It should be noted that these measurements were obtained for a model blockage ratio of 0.03%.

Implicit in Jaffe's discussion[2] is the assumption that the tff sphere drag coefficient values are correct. Whether this is in fact true can be determined by comparing these wind tunnel values with those obtained at the same values of Mach and Reynolds number in actual non-tunnel free flight. These wind tunnel sphere drag coefficient values (tff), which were obtained for a Reynolds number of 2.5×10^5, are compared in Fig. 1 with the corresponding true free-flight values derived from an analysis of such measurements by Miller and Bailey.[3]‡ This comparison shows that for $M_\infty \leq 0.98$, the

Received June 19, 1980.

*Research Engineer, Manchester, Tenn.

†Physical Chemist, Earth Sciences Division.

‡Since the submission of Ref. 3, the work of Giraud[4] has been received. His 20 mm results and the 4 in. data of Zahm[5] (below $M_\infty = 0.6$) have been incorporated with cannon data collected for Ref. 3. These data lead to Fig. 2, which differs only slightly from Fig. 4 of Ref. 3. The most noticeable change is a persistence to higher Mach numbers of the dips at $Re_{\infty d}$ above 5×10^5.